



## Journal of Materials Processing Technology

journal homepage: [www.elsevier.com/locate/jmatprotec](http://www.elsevier.com/locate/jmatprotec)

## Closed-loop control of product properties in metal forming: A review and prospectus

James A. Polyblank<sup>a</sup>, Julian M. Allwood<sup>a,\*</sup>, Stephen R. Duncan<sup>b</sup><sup>a</sup> Department of Engineering, University of Cambridge, Trumpington Street, Cambridge CB2 1PZ, UK<sup>b</sup> Department of Engineering Science, University of Oxford, Parks Road, Oxford OX1 3PJ, UK

## ARTICLE INFO

## Article history:

Received 23 September 2013

Received in revised form 8 March 2014

Accepted 12 April 2014

Available online 24 April 2014

## Keywords:

Flexible forming

Metal forming

Process control

Closed-loop control

Feedback

Sensor

## ABSTRACT

Metal forming processes today operate with astounding productivity, repeatably creating precise parts in high volumes out of the stock sheet and bar products of the upstream metals industries. This achievement has come through decades of development of ever stiffer and more precise tooling used in fast-acting tightly controlled equipment, and yet in the wider context of manufacturing, metal forming processes seem to be less effective: tooling costs are high, and can only be justified by large batch production; the parts made by metal forming are usually not as required for assembly, and must be processed in further downstream machining operations; current processes do not respond well to process disturbances such as tool wear or unanticipated variation in material properties; twenty years of laboratory development of new flexible forming processes has led to little industrial take-up, due to a lack of precision. The missing ingredient in forming which gives rise to these problems is the absence of effective closed-loop control of product properties. The normal practice for blacksmiths and craft workers in former times – using their personal senses to adjust processing in response to evolving conditions – has been forgotten in the pursuit of process rigidity. This paper therefore aims to motivate a new wave of interest in applying closed-loop control of product properties to metal forming processes. A novel framework is developed to show metal forming processes at the heart of an outer control loop, and existing applications are reviewed. Surveys of sensors, actuators and modelling techniques reveal a rich seam of opportunities for new developments, and the paper concludes with some suggestions about near term opportunities for applying closed-loop control of properties to metal forming processes.

© 2014 The Authors. Published by Elsevier B.V. This is an open access article under the CC BY license (<http://creativecommons.org/licenses/by/3.0/>).

## 1. Introduction: today's metal forming makes the wrong shapes

The very earliest metal production involved no losses and no fixed tooling, yet intricate products could be created: a single billet of metal was cast and forged by hand to the required, tailored geometry. Machining – removing material to cut a shape out of the forged product – could begin only once a cutting tool stronger than the metal was created, but almost without conscious choice, the world of manufacturing has become addicted to machining: since the invention of the Bridgeport machining Centre in the 1930s, machine makers have gone on to produce relatively low cost 5-axis (or more) CNC machining centres capable of astonishing precision and speed in converting forged metal into products plus scrap. In

fact, the success of CNC machining has created a strange oblivion in the world of metal forming: our earliest forebears created products of the required shape by forming, with no loss of metal; our standard procedure today is to allow forming to make intermediate products far from the geometry required in final products, and allow CNC machining tools to remove material with precision until the final component is liberated from the approximate shape created by forming. Milford et al. (2011) estimate that one quarter of all steel produced worldwide – and a half of all the metal used to make sheet metal – is cut off in manufacturing and scrapped, never reaching service in the final product.

In order to compete with CNC machining, metal forming processes have had to improve on two criteria: accuracy and flexibility. In order to compete with the accuracy of CNC machining, developers of metal forming equipment have built larger and larger machines, using bigger and stiffer tools to force blanks into the required geometry. Not only is the cost of these tools great, but also the difficulty of predicting the effects of springback leads to a higher cost of tooling due to the need for die try-out. This high

\* Corresponding author. Tel.: +44 01223 338181; fax: +44 01223 332643.  
E-mail address: [jma42@cam.ac.uk](mailto:jma42@cam.ac.uk) (J.M. Allwood).

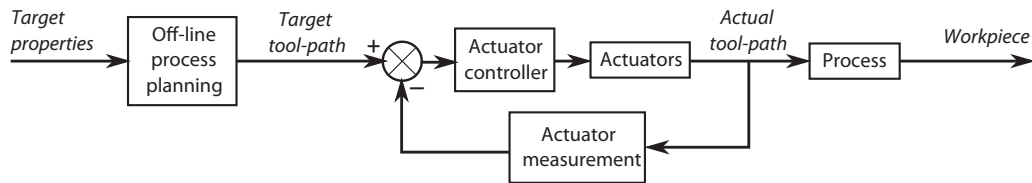


Fig. 1. A system diagram for open-loop control of metal forming.

cost tooling is only economically attractive for large volume production runs. Industries such as aerospace that are inherently low volume producers cannot incur these costs, so instead opt to allow forming to create very approximate geometries from which the required part is liberated by machining with enormous waste of material: the “fly-to-buy” ratio (of material taking off in an aeroplane compared to material purchased) is consistently worse than 10% (Milford et al., 2011).

Competing with CNC machining on flexibility has been the focus of twenty years of innovation since the early 1990s, as illustrated by developments in CNC-servo-presses (reviewed by Osakada et al., 2011), a survey of novel process designs in Japan (Allwood and Utsunomiya, 2006), a survey of possible novel ring-rolling processes (Allwood, 2007) and innovations in process designs for both incremental sheet forming (reviewed by Jeswiet et al., 2005) and incremental bulk forming (reviewed by Groche et al., 2007). Additionally, Allwood (2008) presents a structured search for new metal forming processes highlighting that there is a large number of potential novel process configurations, although he notes that not all will be relevant or commercially viable. However, as yet these processes have had little take-up in industry, primarily because they create products with poor geometric accuracy and high residual stresses.

One of the missing features of these flexible metal forming processes – and one that was inherent to the early manual skills of primitive blacksmiths – is closed-loop feedback control. With eyes, ears and touch, the early blacksmith would adapt his planned approach to forming in response to material behaviour, temperature and tool wear. CNC machining centres can perform well without such feedback for the simple reason that cutting tools affect only the material with which they are in contact. Metal forming, in which the tools influence all of the product properties, and over a much wider area than the zone of contact, requires more sophisticated feedback and compensation – easily provided by human craft workers – but as yet this compensation has received little attention in the development of industrial forming equipment.

Hardt (1993) reviewed applications of closed-loop control of product properties published in the ASME Journal of Dynamic Systems, Measurement and Control and claimed that there was little focus from the dynamics and control community on manufacturing processes or process control – There were only 25 papers in the journal in the preceding 30 years, and only 2 of these related to metal forming, with the rest on machining, welding or casting. More recently, Lim et al. (2008) reviewed closed-loop of product properties in sheet metal stamping processes and found that a great deal of work had been done in this area, but concluded that there was still progress to be made in faster modelling and cost-effective sensors.

The aim of this paper is therefore to provide a more comprehensive and recent review of attempts to introduce closed-loop feedback control into flexible metal forming processes, and attempts to anticipate the potential for future developments in the area, by assessing the building blocks (actuators, sensors and models) already in place that could be deployed in future closed-loop control systems. Section 2 provides a framework for considering how metal forming processes can be examined within the

formalities of existing closed-loop control theory, and anticipates the key components of the system: sensors, actuators, models and control algorithms. Following a survey of preliminary applications published to date, the next three sections of the paper examine these component requirements in turn, to demonstrate that most of the “toolkit” required to implement closed-loop control of metal forming is already available. The final section explores how the topic could develop by predicting how it might apply in processes already under development.

## 2. A theoretical basis for metal forming processes as the heart of closed-loop control systems

Potentially, equipment makers might respond to the challenge of the opening section of this paper by pointing out how much use they already make of closed-loop control. However, the standard control systems of current equipment, while indeed operating within a closed-loop, take no account of the behaviour of the product during processing. Instead, they act to ensure that the equipment’s actuators move precisely according to a “tool-path” or “schedule” planned before processing begins. Indeed, Hardt (1993) highlights that this approach has only an indirect influence on the actual process output, despite being the focus of much of the work in the area of control in manufacturing. This approach to control is illustrated in Fig. 1, which shows what – within this paper – we will call “open-loop” control of metal forming.

Fig. 1 shows the use of feedback control to compare the current position of tools to that planned prior to the operation beginning, and to compensate for any error in position. This form of control system is a mature technology, and most commercial machines sold today will be sold with impressive guarantees on the accuracy of tool positioning during operation.

Typical offline process planning algorithms as shown in Fig. 1 use a model to predict the effect of control actions on the final part. The evolution of  $P$  properties of the part, such as geometry, temperature and grain size, is described by partial differential equations, and solved via a discretisation in space with  $N$  nodes at locations  $\mathbf{x}$ , and recorded as a  $NP \times 1$  state vector,  $\mathbf{q}(\mathbf{x}, t)$  at time,  $t$ . The process model can then be expressed as a first order, vector, ordinary differential equation

$$\frac{d}{dt} \mathbf{q}(\mathbf{x}, t) = \mathbf{f}(\mathbf{q}(\mathbf{x}, t), \mathbf{u}(t), t) \quad \mathbf{q}(\mathbf{x}, 0) = \mathbf{q}^i(\mathbf{x}) \quad (1)$$

where  $\mathbf{q}^i(\mathbf{x})$  is the initial state of the metal at  $t = 0$  and  $\mathbf{f}(\mathbf{q}(\mathbf{x}, t), \mathbf{u}(t), t)$  describes the evolution of the metal’s properties over time under the effect of a set of actuators whose time varying inputs are denoted by the vector  $\mathbf{u}(t)$ . The function  $\mathbf{f}(\mathbf{q}(\mathbf{x}, t), \mathbf{u}(t), t)$  depends upon time explicitly to reflect the possibility that the effect of the actuators may vary over the time span of the processing.

In practice, it is usual to apply a finite number of control inputs to the actuators at discrete time intervals,  $t_k = kT$ , where  $\{k = 0, 1, 2, \dots, K\}$ ,  $K$  is the number of control actions applied during the process and  $T$  is the time between control actions. The continuous time model in Eq. (1) can then be expressed as a discrete time model

that relates the state at time  $t = kT$  to the state at time  $t = (k + 1)T$  by integrating Eq. (1) over the period  $kT < t \leq (k + 1)T$  to give

$$\mathbf{q}_{k+1}(\mathbf{x}) = \mathbf{f}_k(\mathbf{q}_k(\mathbf{x}), \mathbf{u}_k) \quad \mathbf{q}_0(\mathbf{x}) = \mathbf{q}^i(\mathbf{x}) \quad (2)$$

where  $\mathbf{q}_k(\mathbf{x})$  is the state of the part at  $t_k$  and  $\mathbf{u}_k$  describes the control inputs applied to the actuators at time step  $t_k$ . When the workpiece is in state  $\mathbf{q}_k(\mathbf{x})$  and is subject to control action  $\mathbf{u}_k$  (this includes whatever forces, displacements, heat inputs, etc., arising from actuation of all tooling in the process), the process acts to create a new state of the workpiece  $\mathbf{q}_{k+1}(\mathbf{x})$ . The iteration in Eq. (2) could in principle be solved for most known processes. Sufficient analytical knowledge and modelling capability exists to make plausible predictions of the evolution of the state, for example through finite element methods. However, the form of Eq. (2) is deceptively simple, and disguises the exceptional computational burden of solution: predicting the evolution of  $\mathbf{q}_k(\mathbf{x})$  for known actuator inputs  $\mathbf{u}_k$  may take several weeks with current computing power.

The aim of forming operations, is to ensure that at the end of the process (i.e. after  $K$  control actions), the final state of the process matches  $\mathbf{q}^d$ , the target state required by the customer, so that

$$\mathbf{q}_K(\mathbf{x}) = \mathbf{q}^d \quad (3)$$

In practice, it is unlikely that any process can satisfy this constraint exactly. Instead, the aim is to minimise the difference between the final state and the desired state, where the difference is usually expressed as the quadratic error

$$\|\mathbf{q}_K(\mathbf{x}) - \mathbf{q}^d(\mathbf{x})\|_2 \quad (4)$$

This is referred to as a terminal cost as it is the difference between the final state (at interval  $K$ ) and the desired state. Sometimes, the states and the control inputs must remain close to some desired trajectory during processing (for example to avoid large control actions), in which case the error in the intermediate intervals  $\{k = 1, 2, 3 \dots, K - 1\}$ , and the error in the control inputs are added to the terminal cost to give

$$\|\mathbf{q}_K(\mathbf{x}) - \mathbf{q}^d(\mathbf{x})\|_2 + \sum_{k=1}^{K-1} [\|\mathbf{q}_k(\mathbf{x}) - \mathbf{q}_k^d(\mathbf{x})\|_2 + \lambda \|\mathbf{u}_k - \mathbf{u}_k^d\|_2] \quad (5)$$

where  $\mathbf{q}_k^d(\mathbf{x})$  describes the desired trajectory of the states,  $\mathbf{u}_k^d$  denotes the desired control inputs and  $\lambda$  is used to adjust the weighting applied to the cost on the control inputs.

All metal forming processes operate subject to both machine constraints (for example the range, speed or acceleration of actuators) and material forming limits. Either form of constraint can be expressed as a vector inequality with the form

$$\mathbf{p}_k(\mathbf{q}_k(\mathbf{x}), \mathbf{u}_k) \leq 0 \quad (6)$$

Constraints can depend upon the inputs only, for example when the range of allowable inputs that can be applied to actuators is limited, or on the state only, such as when there are forming limits that restrict the amount of deformation that can be achieved by each control action. The constraints can also depend upon both control input and state, for example in a flexible sheet forming process, deformation occurs only when the tool is in contact with the sheet, and this implies a constraint on the control input dependent on the current sheet geometry.

Eqs. (2), (5) and (6) can now be combined to define open-loop tool-path planning as a standard optimisation problem:

$$\begin{aligned} \min_{\mathbf{u}_0 \dots \mathbf{u}_{K-1}} & \left\{ \|\mathbf{q}_K(\mathbf{x}) - \mathbf{q}^d(\mathbf{x})\|_2 + \sum_{k=1}^{K-1} [\|\mathbf{q}_k(\mathbf{x}) - \mathbf{q}_k^d(\mathbf{x})\|_2 + \lambda \|\mathbf{u}_k - \mathbf{u}_k^d\|_2] \right\} \\ \text{subject to} & \quad \mathbf{q}_{k+1}(\mathbf{x}) = \mathbf{f}_k(\mathbf{q}_k(\mathbf{x}), \mathbf{u}_k) \\ & \quad \mathbf{q}_0(\mathbf{x}) = \mathbf{q}^i(\mathbf{x}) \\ & \quad \mathbf{p}_k(\mathbf{q}_k(\mathbf{x}), \mathbf{u}_k) \leq 0 \end{aligned} \quad (7)$$

The solution to (7) determines the set of control inputs, typically called the “tool-path” or “production schedule” that should be followed to create the target product. In practice, most forming processes today use a control system, such as that illustrated in Fig. 1, to ensure that the actuators follow a target tool-path. In some cases where the actuator tool-path has a simple form, such as in the preset of actuators prior to commencing flat-rolling, the actuator settings are determined by a model using an algorithm of the form of (7). However, for processes such as metal spinning in which the tool-path is much more complex, the computational cost of (7) is as yet far too great, so the tool-path is determined by a combination of operator experience and iterative trials.

The weakness of this approach is that it aims to match the actuator settings  $\{\mathbf{u}_k: k = 0, 1, \dots, K - 1\}$  to a planned sequence, rather than aiming to match the final state of the product,  $\mathbf{q}_K(\mathbf{x})$  to the desired state  $\mathbf{q}^d(\mathbf{x})$ , as required by the customer. In principle, if the process model is perfect, the optimal tool-path should achieve this desired final state, but in reality this is unlikely for three reasons:

- **Model uncertainty:** The model,  $\mathbf{f}$ , defined in Eqs. (1) and (2) is in practice unlikely to predict the exact behaviour of the process, particularly if an approximate form of  $\mathbf{f}$  is used to reduce solution times. In addition, some of the parameters in the model, such as yield stress, may not be known exactly. The model will be based on nominal values for the uncertain parameters, but the true values may lie within a range around these nominal values. The prediction of forming limits within the constraints of Eq. (6) will also, in practice, be imperfect.

Uncertainties can be included in the process model of (2), for example using an additive expression,

$$\mathbf{q}_{k+1}(\mathbf{x}) = \mathbf{f}(\mathbf{q}_k(\mathbf{x}), \mathbf{u}_k) + \Delta(\mathbf{q}_k(\mathbf{x}), \mathbf{u}_k) \quad (8)$$

where the uncertainty  $\Delta$  is usually defined as belonging to a set of possible model errors  $\delta$ . For example, the yield stress might take any value from the set defined by the range  $\sigma_Y \leq \sigma_y \leq \bar{\sigma}_Y$  where  $\sigma_Y$  and  $\bar{\sigma}_Y$  define the minimum and maximum possible values. An extension to the solution of (7) could anticipate the likely consequences of the model uncertainty in creating a predicted distribution for the terminal cost of Eq. (4).

- **Disturbances:** External disturbances, such as variability in lubrication, tooling wear, or variation in operating temperatures, will cause variation in process performance compared with what is modelled. Disturbances can also be included in the model, for example by extending the version in (8) to

$$\mathbf{q}_{k+1}(\mathbf{x}) = \mathbf{f}(\mathbf{q}_k(\mathbf{x}), \mathbf{u}_k) + \Delta(\mathbf{q}_k(\mathbf{x}), \mathbf{u}_k) + \mathbf{d}_k(\mathbf{x}) \quad (9)$$

The disturbance  $\mathbf{d}_k(\mathbf{x})$  could be defined statistically, for example, by the mean  $\mu$  and the covariance matrix  $\Sigma$  of a (vector) Normal distribution,  $\mathbf{d}_k(\mathbf{x}) \sim N(\mu, \Sigma)$  and as above, it would be possible to predict the effect of these disturbances on the terminal cost of Eq. (4).

- **Controllability:** Most forming machines are designed for a specific purpose, and it is unlikely that they can achieve all desired states perfectly – due to limitations in actuation or tooling. For example, in a flexible sheet forming processes it is unlikely that the actuators can create any arbitrary geometry anywhere within the workpiece. Any state that cannot be affected by the actuators within a finite time period is said to be *uncontrollable*. Within the literature on control systems, most discussions of controllability focus on dynamic controllability (Astrom and Murray, 2008), but in sheet forming, the *spatial* controllability of the process also needs to be considered (Duncan and Bryant, 1997). The concept of spatial controllability comes from the control of distributed parameter systems (Curtain and Zwart, 1995) and describes the ability of the process to achieve specific spatial shapes, which depends upon the location and the spatial response

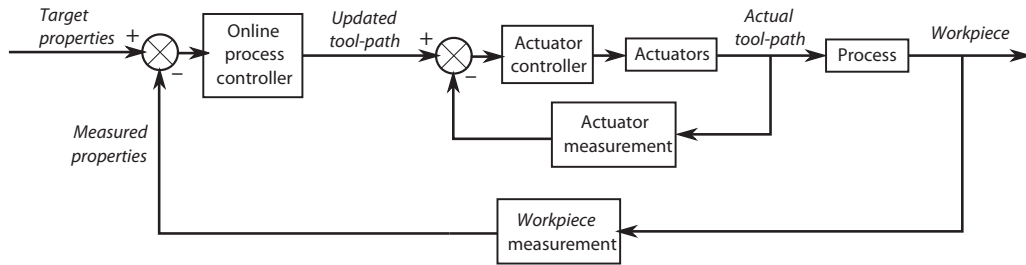


Fig. 2. A system diagram for closed-loop control of metal forming.

of the actuators in the process. The solution to (7) will cope with uncontrollable states by minimising the terminal cost subject to the constraints which can be reflected in the form of (6). Alternatively, an inverse form of (7) could be solved to define the actuation and tooling required to reduce the terminal cost to some target value.

It would therefore be helpful to find a different approach from that of Fig. 1 for developing tool paths in metal forming processes that is more robust to modelling errors and disturbances. In past times, the blacksmith did not plan his actions in advance, but developed them during production in reaction to feedback from his own senses. Learning from this approach, if we were able to install sensors within the forming process to monitor the state of the workpiece during processing, we can imagine a different form of tool path design using closed-loop control, as illustrated in Fig. 2. This approach, which updates the tool path on the basis of the current state of the part is the aspiration of the work reviewed and previewed in this paper: if only we could monitor the whole state of the workpiece during processing, and if only – like the blacksmith – we had sufficient actuation and intelligence to adapt our next actions to the current state of the product and the tools, we could then adjust our plans for actuation to guarantee that the product does eventually match precisely what we always intended for it.

Fig. 2 introduces two changes to Fig. 1: a means to measure the workpiece state during processing, and an online process controller in place of the previous offline process planning expressed as Eq. (7). A wide range of sensors exists to measure the workpiece state, and will be surveyed in Section 4 of the paper.

An ideal forming process would allow complete and perfectly accurate measurement of the workpiece state  $\mathbf{q}_k(\mathbf{x})$  at every time step  $k$ . In reality, it is more likely that only part of the workpiece can be measured at any time, and often, sensors record measurements that are themselves functions of the state, and possibly of the current actuation as well. For example, although it is usually not possible to measure the microstructure of the metal directly, if the temperature of the part is measured, then information about the microstructure can be inferred. Equally, measurements of workpiece geometry may be influenced by its elastic deflection due to current actuation, known as springback.

The workpiece state is therefore predicted by a model based observer  $\mathbf{h}$  to generate a state estimate  $\hat{\mathbf{q}}_k(\mathbf{x})$  based on measurements  $\mathbf{y}_k$  created by whatever sensors are available, and current actuation  $\mathbf{u}_k$  using

$$\hat{\mathbf{q}}_{k+1}(\mathbf{x}) = \mathbf{h}(\hat{\mathbf{q}}_k(\mathbf{x}), \mathbf{u}_k, \mathbf{y}_k) \quad (10)$$

starting from an initial estimate  $\hat{\mathbf{q}}_0(\mathbf{x}) = \hat{\mathbf{q}}^i(\mathbf{x})$ , where the index,  $i$ , is used to denote “initial”.

As with the open loop controller of Fig. 1, two problems limit the quality of this state estimate:

- **Observability:** The measurement system used to identify the current state should ideally be designed so that a change in any of the states must be detected by at least one of the sensors. Any state whose change cannot be detected by any of the sensors is said to be unobservable. Clearly it is a requirement of the design of effective closed-loop control systems for metal forming that the actuation and measurement systems are designed so that the states of all points of interest within the part are both controllable and observable to the extent required to minimise the terminal cost to an acceptable level.
- **Sensor noise:** Measurements are susceptible to sensor noise, which means that it is not possible to determine whether a variation that is measured by a sensor is actually a change in the state, or whether the variation is due to noise. However, if the statistics of the disturbances on the state, as defined in (9), and the random effects of the noise, then the observer in (10) can be designed to provide an estimate of the state that minimises the expected value of the difference between the estimated state and the actual state (Astrom and Murray, 2008).

Armed with sensors and the state observer of (10), the control system design of Fig. 2 now leads to a closed-loop version of the open-loop optimisation statement of (7). The optimal set of control actions can be determined iteratively using

$$\begin{aligned} \min_{\mathbf{u}_{k'} \dots \mathbf{u}_{K-1}} & \left\{ \|\hat{\mathbf{q}}_K(\mathbf{x}) - \mathbf{q}^d(\mathbf{x})\|_2 + \sum_{k=k'}^{K-1} [\|\hat{\mathbf{q}}_k(\mathbf{x}) - \mathbf{q}_k^d(\mathbf{x})\|_2 + \lambda \|\mathbf{u}_k - \mathbf{u}_k^d\|_2] \right\} \\ \text{subject to} & \quad \hat{\mathbf{q}}_{k+1}(\mathbf{x}) = \begin{cases} \mathbf{f}_k(\hat{\mathbf{q}}_k(\mathbf{x}), \mathbf{u}_k) & \text{for } k = k' + 1, k' + 2, \dots, K \\ \mathbf{h}(\hat{\mathbf{q}}_k(\mathbf{x}), \mathbf{u}_k, \mathbf{y}_k) & \text{for } k = 0, 1, \dots, k' \end{cases} \\ & \quad \hat{\mathbf{q}}_0(\mathbf{x}) = \hat{\mathbf{q}}^i(\mathbf{x}) \\ & \quad \mathbf{p}_k(\mathbf{q}_k(\mathbf{x}), \mathbf{u}_k) \leq 0 \end{aligned} \quad (11)$$

Although (11) has a similar form to the earlier statement in (7), this minimisation is different because it is applied to control actions over the period from  $t_{k'}$  to  $t_{K-1}$  rather than the whole of the process, and the update of the process model uses the estimate of the current state  $\hat{\mathbf{q}}_{k'}(\mathbf{x})$  obtained from the measurements rather than the modelled state. In applying this algorithm within the closed-loop system of Fig. 2, having solved (11) to work out the optimal sequence of control actions  $\{\mathbf{u}_k : k = k' \dots K-1\}$ , only the first element of this sequence,  $\mathbf{u}_{k'}$  is applied to the process, before taking another measurement of the state at the next time step to generate a new estimate of the state,  $\hat{\mathbf{q}}_{k'+1}(\mathbf{x})$ . The minimisation is then repeated to give the optimal sequence of control actions over the (shorter) interval from  $t_{k'}$  to  $t_{K-1}$ , where the new estimate of the state based on the measurements taken at time  $t = (k' + 1)T$  is used as the starting point for the process model. This idea of performing a repeated set of optimisations using an estimate of the current state is a discrete form of Model Predictive control (MPC) (Maciejowski, 2000).

The terminology used here, and most of the examples in this report, relate to closed-loop control used during the production of single parts. However, the same theory can easily be extended



to run-by-run control method as Rzepniewski and Hardt (2008) did for a flexible stretch forming process. In this case,  $k$  is the part number,  $\mathbf{u}_k$  is the actuator controls used to produce the part, and  $\mathbf{q}_k$  to the state of that single finished part. The actuator settings would then be modified for the next part. This approach might be used if either the process model or the observer is too slow to be used online, or if the state cannot be measured online.

The process model that is used as the basis of the minimisation in (11) does not include the model uncertainty, the disturbance and the sensor noise because these effects are all unknown. While it is possible to design control systems that accommodate these effects directly by minimising the difference between the final state and the desired state in the presence of uncertainty, disturbances and noise (Green and Limebeer, 2012), because the controller focuses on the worst possible effect, this tends to produce very conservative controllers that perform poorly. Instead, the calculation of the control inputs in (11) is based on the nominal model of the process in (2) and the feedback provided by the measurements and the estimates of the state from the observer  $\mathbf{h}$  provides robustness against process disturbances. In addition, the use of the feedback also provides robustness against model error, so unlike the approach of Eq. (7), Eq. (11) specifically allows the use of a less accurate model of process  $\mathbf{f}$ , and this allows great reductions in the computational burden of the optimisation. Eventually if a sufficiently fast model can be found then, just as with the blacksmith of old, the system in Fig. 2 can operate on-line.

Applying the control inputs that are the solution to the optimisation problem in (11) does not guarantee that the process will remain stable. One definition of stability is that for a bounded (i.e. finite) set of inputs, the output must also remain bounded (Green and Limebeer, 2012). The process that we are considering uses a finite number of steps (i.e.  $K$  steps) and since we can only apply finite inputs, the output from a finite number of steps cannot become unbounded. However, the effect of instability can be observed in oscillations in the deformations applied to the sheet at successive control actions or when adjacent actuators apply opposing changes (Duncan, 1989). Although the effects of instabilities are usually masked by constraints that prevent large inputs being applied to the actuators, the stability of the feedback system must be checked for all possible model uncertainties, before the controller is implemented on the process (Maciejowski, 2000).

Fig. 2 and Eq. (11) define the ambition for applying closed-loop control to metal forming processes that motivates this paper. The next section reviews the first attempts published to date to implement closed-loop control in different metal forming processes. There are relatively few such publications, but the structure of Fig. 2 allows us also to look ahead to how this subject might grow: the conversion of the current operation of metal forming in Fig. 1 to the future proposal of Fig. 2 requires discussion of three themes – which are the agenda of Sections 4–6 of the paper: What sensors could be used to monitor the workpiece during process operation? What actuators can be introduced into metal forming processes to recreate the flexibility and responsiveness of the blacksmiths of the past? What approaches can be used to create models of sufficient accuracy with sufficient speed to allow online operation of the optimisation in Eq. (2)?

### 3. Applications of closed-loop control of product properties in metal forming

Published reports of the application of closed loop control of product properties in metal forming, as defined in Fig. 2, are summarised in Table 1.

In these applications, closed loop control has been used to address errors in geometry, residual stress and material

properties and also to avoid defects. According to Lange (1985) surface error is also an important final product property, but no examples of surface errors being addressed by closed-loop control have been identified.

Out of these applications, closed loop control has been used most extensively to control errors in geometry (including springback), with this being the focus in 8 out of the 11 applications, and with large reductions in error reported in many of these cases. Residual stress was the aim of just one application, flat rolling, even though this has been the focus of much research since the 1970s. This is probably due to the relative ease with which residual stress can be observed and controlled in strip rolling (Sheppard and Roberts, 1973, review this work). A single application aimed to avoid defects in deep drawing, with the blank holder force controlled based on measurements of punch force, blank holder friction force or flange draw-in. Although this approach is robust against external disturbances, if additional flexibility were added (for example, in the incremental deep drawing process developed by Shima et al., 1999), then experimental trajectories would have to be determined experimentally, adding lead time and setup costs. Only one application addressed the control of material properties. Recker et al. (2011) propose a vision for incremental forging where grain size, and therefore material properties, can be controlled. However, although Recker et al. have demonstrated a working observer which can determine the grain size in the bulk of the product, they have not yet implemented a controller.

### 4. State observation – measuring product properties

Since the time of Henry Ford, all manufacturers have measured properties of concern to customers as part of their quality assurance process and this measurement has become increasingly automated. As a consequence of this, a broad range of sensors and observers now exist for offline measurement of product properties. Many of these have been adapted to provide online measurement and Section 4.1 presents an overview of available options for their use in closed-loop control of product properties. However, the value of using a set of sensors depends on their arrangement around the workpiece, and this is examined in Section 4.2.

#### 4.1. Sensors and observers

Tables 2–6 present a survey of sensors that could be used in metal forming processes for measuring displacement, surface properties, force, temperature, microstructure, defects, residual stresses and materials properties. The tables report the domain over which the properties can be measured (point, line, surface of volume) and the sensors are classified as contacting or non-contacting (as this may limit their applicability for on-line control). References are given to examples where the sensor is already used in real time in a metal forming or related process. Descriptions of each sensor or technique are given in Appendix A. Readers wishing for a more detailed review of force, temperature and displacement sensors might refer to Shieh et al. (2001).

Geometry, residual stresses and surface properties can be measured directly by the sensors listed in these tables, but where spring back occurs after unloading the product from the process, the measured geometry may not be that perceived by the end-user. This problem may be overcome in batch production by unloading the product from the machine, or in continuous production by running the material out of the loaded zone prior to measurement. However, both approaches lead to a time-delay in feeding back measurements to the control system. An alternative method is to measure the loaded geometry and use an observer to estimate the unloaded geometry. Hardt et al. (1982) and Hardt and Hale

**Table 1**  
Published applications of metal forming processes with closed loop control of product properties.

Process	Error signal	Observed product property, $x$	Controlled action, $u$	Modelling approach	Reported improvement
Three-roll bending and straightening	Springback error in unloaded curvature	Unloaded curvature (by measuring tool force and loaded curvature)	Displacement of central roller to vary bending moment	Integrator (i.e. integrated error to determine control action)	In bending, curvature errors <3% (Hardt et al., 1982); in straightening, lateral deflection reduced by 53–91% over 300 mm (Hardt and Hale, 1984); in bending of profiles, error reduced by factor of 10 (Yang et al., 1990)
L-bending	Springback error in unloaded bend angle	Unloaded bend angle	2D position of bending tool, to allow a variable overbend	Neural network (using a database of previous results)	Bend angle error reduced from 4° to 0.5° in 90° bend (Yang et al., 1998)
Channel forming	Springback error in unloaded bend angles; tearing	Punch force	Blank holder force (BHF)	Neural network (using a database of previous results)	Springback reduced from between 1° and 8.5° for constant BHF to being consistently around 1° with controlled BHF in an 56° bend in aluminium, even with variable friction conditions (Sunseri et al., 1996). Further reduced to 0.2°–0.6° using neural network to determine BHF (Cao et al., 2000). Also shown to be effective with steel channels (Viswanathan et al., 2003)
Roll forming of U-profiles	Springback error in unloaded bend angles	Unloaded bend angles	Bend angle of final set of rollers	Groche et al. (2008) use a Smith-Predictor to compensate for the delay between actuation and sensing.	Bend angle error reduced to 0.2°, compared to DIN regulation of 1.25° (Groche et al., 2008)
Multi-axis bending and twisting	Springback error in unloaded curvatures and twist	Unloaded curvature and twist	2D position, and 3D rotation of movable die	Luo et al. (1996) use an approximate, dynamic transfer function in Laplace space, derived from classical beam theory with elastic-perfectly-plastic material model. Sun and Stelson (1997) and Li et al. (2007) use adaptive models.	Errors in curvature reduced from 50% to 10% (Luo et al., 1996; Sun and Stelson, 1997)
Stamping with a matrix of punches	Springback error	Unloaded shape	z-Position of each punch in a matrix	Estimated springback based on difference between tool shape and resulting part shape.	Error in depth reduced from 13% to 2% (Hardt and Webb, 1982); more recently from 4.2 mm to 0.25 mm (Li et al., 2007)
Incremental sheet forming	Springback error	Unloaded shape (still clamped in blank holder)	3D position of tool	Allwood et al. (2009) use an impulse response approach. Hao and Duncan (2011) linearise about a planned toolpath.	Error in depth reduced from up to ±3 mm to ±0.2 mm in a 25 mm depth truncated cone (Allwood et al., 2009; Hao and Duncan, 2011)
Laser bending	Springback error after cooling	Shape after cooling	Position of laser on surface	Edwardson et al. (2004) used contours of error between target and measured shape height as a path for the laser.	Error in height reduced from 8 mm to 2.5 mm in 25 mm high dome (Edwardson et al., 2004)
Deep drawing	Defects (wrinkling and tearing)	Punch force; friction force on blank holder; flange draw-in; wrinkle height; part wall stress	Total BHF, local BHF and/or draw bead penetration	Trajectories found by experiment/FE simulations. BHF controlled using various approaches reviewed by Lim et al. (2008), including transfer function; proportional-integral controllers with feedforward; neural network.	Punch force control acts to “lower the sensitivity of the deep-drawing process to undesirable effects” (Michler et al., 1994); Achieved optimal failure height, independent of initial BHF while for constant BHF, failure height dropped off quickly as BHF moves from optimum (Hardt and Fenn, 1993); “Production reliability is notably increased” (Siegert and Ziegler, 1997); Only useful in regions where wrinkling will occur and will not avoid tearing – needs to be combined with another measurement (Siegert and Ziegler, 1997); reduced springback and improved part quality while die spotting can be

Table 1 (Continued)

Process	Error signal	Observed product property, x	Controlled action, u	Modelling approach	Reported improvement
Strip rolling	Residual stress caused by thickness variations	Thickness variation or residual stress	Setting of roll bending jacks to vary the roll deflection	Response matrix of actuators is measured empirically and used in controller.	omitted (Blaich and Liewald, 2008); prevented tearing when a systematic error was introduced, which caused tearing in the open-loop case (Endelt et al., 2013). Flatness error reduced to 40% of uncontrolled value with 2 actuators (Bravington et al., 1976); reduced to 5% with 10 actuators (Duncan et al., 1998).
Ring rolling	Form errors, corner errors, temperature and residual stress, material properties, stability.	Outer diameter, ring centre	Position of working roller	Yun and Cho (1985) use a PID controller, tuned based on a slab-style, non-linear analytical model from Hawkyard et al. (1973). Most industrial controllers use a controller based on Koppers's (1987) kinematic model, but details are not published. Xiaokai and Lin (2011) simply continue to feed the tool until desired diameter reached, then stop. Recker et al. (2011) share a vision for a man-in-the-loop system, but yet to carry out experiments.	Yun and Cho (1985) reduce error from 1.26 to 7.20 mm in a non-optimised controller to 0.31 mm in their controller in a 253.44 mm ring. Xiaokai and Lin (2011) achieved errors of ~0.1% in outer diameter achieved.
Incremental forging	Material property uncertainty	Grain size (predicted by modelling, based on measured geometry and surface temperature)	Rotation and position of workpiece; position of punch.		No experiments yet carried out with control system (Recker et al., 2011)

(1984), studying three-roll bending and straightening, measured tool forces and displacement throughout process operation to infer workpiece moment and curvature, and hence deduce the gradient of the elastic part of the moment-curvature curve. This was used to predict the change in curvature on unloading (springback), and hence allow compensation.

Defects, such as cracks and wrinkles, can also be measured directly using the sensors in Table 6. However, once a defect is already present in the workpiece, it is often too late to change future control actions to remove it. Instead, a constraint could be used to prevent the formation of a defect, for example based on accumulated damage. Damage, and many other features of workpiece microstructure cannot be observed directly, but could be estimated by an observer.

The estimation of *material properties* arising from particular boundary conditions applied to specific metals has been the main

pre-occupation of material scientists in the past 30 years or more. Increasingly this allows the production of bulk or distributed material properties from surface measurements of temperature and geometry. Recker et al. (2011) apply such models in an observer to estimate interior grain size from measurements of surface displacement and temperature in incremental forging.

Table 7 illustrates how the outputs from the sensors in Tables 2–6 could be used by a state observer to create an estimate of the state or product properties of the workpiece.

The evidence of this section suggests that, although the examples of closed-loop control discussed in Section 3 were largely focused on geometric springback, a much wider range of sensors could be applied in future online control of product properties in metal forming. The coupling of sensors with models of microstructure evolution demonstrated by Recker et al. (2011) illustrates how the use of observers could in future greatly extend the range of

Table 2

Sensors that could be used to measure dimensional errors in metal forming processes (measurement domain characterised as P=point, L=Line, S=surface, V=volume, with CL indicating contactless measurement).

Sensor/technique	Domain	Example real time applications
Mechanical follower	P	Bravington et al. (1976) measure thickness in flat rolling. Duncan et al. (2000) use more followers to get better resolution.
Direct Induction	P(CL)	Cao et al. (2002) describe a sensor for measuring the draw in of the flange in deep drawing. Mahayotsanuna et al. (2009) apply this online.
Laser Line Triangulation	L(CL)	Groche et al. (2008) measure the angles in U-channel rolling
Silhouette (single)	L(CL)	Not yet used, but requires a light with a camera on opposite sides of the part. Fast image processing would be able to identify part shape.
Boroscope	L(CL)	Hamedon et al. (2012) use a boroscope to monitor the edge of the sheet in a shrink flanging operation.
Laser scanning	S(CL)	Recker et al. (2011) measure the workpiece in incremental forging
Stereovision Camera	S(CL)	Allwood et al. (2009) measure workpiece geometry in incremental sheet forming
Stereoscopic boroscope	S(CL)	Hamedon et al. (2012) use multiple boroscopes to build up a 3D image of the sheet surface during a stamping operation.
X-ray Tomography	V(CL)	Nguyen-Thi et al. (2012) measure the internal structure of a part during casting. Takes ~20 s to build 3D image.

**Table 3**  
Sensors that could be used to measure surface roughness and defects in metal forming processes (measurement of Z = distance from sensor, R = roughness, D = Defects; measurement domain characterised as P = point, L = Line, S = surface, with CL indicating contactless measurement).

Sensor/technique	Measure	Example real time applications (where found)
Stylus Scanners	Z, L	Could potentially include atomic force microscopy <a href="#">Frade et al. (2012)</a> measure surface profiles from a working distance of 90 mm at 57,600 pts/s.
Optical Surface Measurement	Z, P(CL)	
Capacitance Techniques	Z, P(CL)	<a href="#">Sautome and Okamoto (2001)</a> measure the shape of a ~1 mm part in micro-incremental forming <a href="#">Jeong et al. (2006)</a> determines when a layer of material has been removed in planarization.
Stereo Optical Microscopy	Z, S(CL)	
Scanning Electron Microscopy	Z, S(CL)	
Acoustic Emissions Measurement	R, L	<a href="#">Jeong et al. (2006)</a> determines when a layer of material has been removed in planarization, by measuring the frictional force to move the polishing head.
Inductive Technique	R, S(CL)	
Impedance/Skin Effect Technique	R, S(CL)	
Friction Measurement	R, S	
Liquid-penetrants Technique	D, S	

**Table 4**  
Sensors that could be used to measure forces in metal forming processes (measurement domain characterised as P = point, S = surface; all of these sensors require contact).

Sensor/technique	Domain	Example real time applications
Load cell	P, S	These are widely applied to measure tool forces, for example <a href="#">Yoneyama and Tozawa (1990)</a> in forging, including use of an array of load cells to measure die filling.
Piezoelectric (PE) Force Sensor	P	<a href="#">Jeong et al. (2006)</a> measure friction force in a planarization.
Piezoresistive (PR) Force Sensor	P	Piezoresistive sensors could be used in a similar way to piezoelectric sensors. They are already used in strain gauges in accelerometers.

**Table 5**  
Sensors that could be used to measure temperature in metal forming processes (measurement may be D = discrete, C = continuous, B = binary; measurement domain characterised as P = point, S = surface, with CL indicating contactless measurement).

Sensor/technique	Measure	Example real time applications (where found)
Thermocouple	C, P	<a href="#">Yoneyama and Tozawa (1990)</a> measure workpiece surface temperature in a forging process.
Bimetallic thermometers	C, P	Used for real-time temperature measurement in fluids.
Fibre-optic temperature sensors	C, P	
Integrated-circuit (IC) temperature sensors	C, P	Soap (which changes state at a single temperature) is often used in craft work to indicate the annealing temperature of aluminium. Monitoring of similar phase-changing coatings could be automated.
Irreversible/change-of-state temperature sensors	B, P(CL)	
Liquid crystal temperature indicators	D, P(CL)	As above, could be used with optical sensors. Can change state at around 10 discrete temperatures
Liquid-in-glass thermometers	C, P	<a href="#">Recker et al. (2011)</a> measure surface temperatures in a workpiece in open-die incremental forging.
Piezoelectric (PE) temperature sensors	C, P	
Thermistors	C, P	
Thermostats	B, P	
Optical pyrometer	C, S(CL)	

**Table 6**  
Sensors that could be used to measure defects, microstructure, residual stresses and materials properties in metal forming processes (measurement of G = grain size, M = microstructure, D = Defects,  $\rho$  = density, E = residual strain, F = features of plastic deformation; measurement domain characterised as S = surface (and in some cases subsurface), V = volume, with CL indicating contactless measurement).

Sensor/Technique	Measure	Example real time applications (where found)
Magnetic-particle inspection technique	D, S	<a href="#">Yogo et al. (2009)</a> monitors surface microstructure during hot deformation <a href="#">Pasadas et al. (2011)</a> describes a handheld device to detect defects in conductive plates. Results are shown on a screen in real-time.
Thermography	D, S(CL)	
Optical Microscopy	G, S(CL)	
Eddy-current inspection techniques	D, V(CL)	
Induction Spectroscopy	M, V(CL)	<a href="#">Davis et al. (2011)</a> use induction spectroscopy to monitor the phase transformation from austenite to ferrite during online processing of steel.
Radiography and Tomography	Dp, V(CL)	<a href="#">Nguyen-Thi et al. (2012)</a> use X-ray tomography to measure the internal structure of a part during casting. Takes ~20 s to build 3D image.
X-ray Diffraction (XRD)	GE, V(CL)	<a href="#">Gururajan and Ogale (2012)</a> apply XRD to measure crystalline orientation in polymer film extrusion
Ultrasonic/Acoustic methods	DEG, V(CL)	<a href="#">Takada et al. (2011)</a> use on-line ultrasound scanning to detect non-metallic inclusions in metal sheet rolling
Acoustic-emission sensing	DF, V(CL)	<a href="#">Liang and Dornfeld (1990)</a> used acoustic emissions sensing which detects aspects of plastic deformation to anticipate fracture in stretch forming and deep drawing.



**Table 7**

Measurable outputs, models that could be used in a state observer, and states (product properties) relevant to metal forming.

Measurements	Models	States
Geometry	Deformation model	Geometry
Surface temperature	Heat transfer model	Stress, strain rate and temperature throughout product
Tool force	Microstructure evolution model	Residual stress
Residual stress (near surface)	Damage model	Hardness
Grain size/composition (near surface)		Toughness
Defects (Cracks, wrinkles, etc.)		Damage
Surface properties (roughness, defects, etc.)		Surface properties (roughness, defects, etc.)
		Grain size/composition

properties included in the target state of controlled metal forming processes.

#### 4.2. Estimating the product state from partial sensing

Many of the sensors listed in Tables 2–6 operate only at points or along lines, so an estimate of the state of the whole workpiece must be interpolated from partial measurements, for example by scanning, or the use of multiple sensors. This interpolation may introduce errors into the estimated state, and the errors are influenced by the design of the sensing system. The challenge of creating the most information possible about the state of the workpiece from partial sensing is illustrated in this section with reference to closed-loop control of profile in strip rolling.

Two approaches have been used to measure strip profile on-line: Wellstead et al. (2000) describe use of a scanning sensor downstream of the mill, which provides measurements along a zig-zag line along the sheet. However, profile errors between each line of the zig-zag will be undetected, so regardless of actuator responsiveness, the control system cannot eliminate errors with wavelengths shorter than the gap between profile scans. Alternatively, Bravington et al. (1976) describe the use of an array of sensors distributed across the width of the strip. This eliminates the difficulty of observing higher frequency profile errors in the rolling direction, but is restricted in the cross-direction to measuring errors with wavelength greater than the spatial separation of the sensors.

The performance limits of sensors and sensory arrays can be analysed by characterising possible error signals with an appropriate set of (orthogonal) basis functions. For time-domain signals, this is often achieved using Fourier transforms, but for the spatial measurements required in metal forming, different approaches are required. Bravington et al. (1976) demonstrate a simple approach, characterising cross-directional sheet thickness errors in strip rolling, as a sum of constant, linear, quadratic and variation and relating these errors to the capability of the available actuators. A more general approach taken by Duncan et al. (1998), uses a basis set of Chebyshev Polynomials of increasing order, to relate sensor capability to available actuation. Analysis of this type assists with the positioning of sensors, and specification of the performance limits of the closed-loop control system.

### 5. Actuators for property control in metal forming

If an appropriate sensor and observer has been used to estimate the discrepancy between the actual and target state, a closed-loop control system can update the control actions and attempt

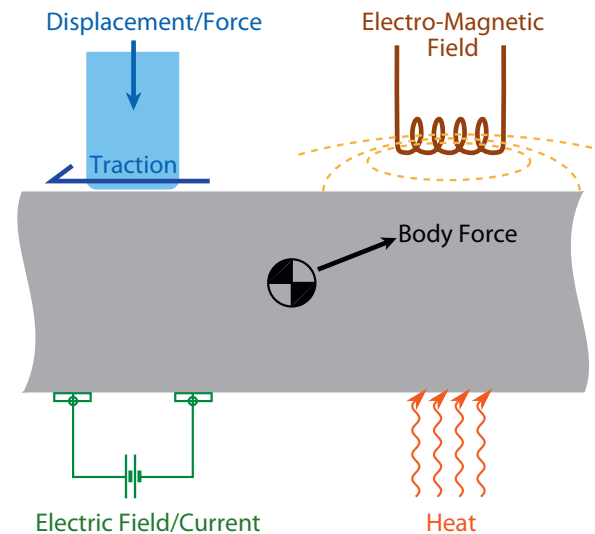


**Fig. 3.** The boundary conditions which can be applied in metal forming processes.

to reduce the error. In most current metal forming processes, actuators are used only to do mechanical work or apply heat, but more broadly could include any device to apply boundary conditions that influence product properties. The range of possible actuators is reviewed in Section 5.1, and, by analogy with the use of arrays of sensors discussed in Section 4.2, the influence of actuator positioning is considered in Section 5.2.

#### 5.1. A catalogue of actuators

Fig. 3 illustrates the types of boundary condition that may be applied in metal forming processes. Actuators already exist to apply all of these boundary conditions, and surveys and catalogues exist in many forms. For example, Huber et al. (1997) review linear mechanical actuators which can apply displacement or force boundary conditions. Their results are organised by maximum actuator stress against maximum actuator strain (the extension of an actuator as a fraction of its initial length) and are recreated in Fig. 4.

Actuators exist, to influence all of the product properties that can be measured using the sensors reviewed in Section 4: dimensional error, surface properties, material properties and damage. However, within the bulk of the workpiece, only body forces can be applied, by gravity or by inertial effects. Electromagnetic fields penetrate only a short distance into the workpiece: Zhang et al. (1995) report that high frequency fields penetrate only to a shallow skin depth while at low frequency, the electromagnetic field although penetrating further provides much less force. Similarly, Clark and Sutton (1996) note that microwaves act only at the workpiece surface, so cannot create internal heating except by diffusion from the surface.

For sheet forming processes with thin workpieces, this constraint is not limiting – and examples of laser-assisted forming (for example, Geiger and Vollertsen's (1993) work on laser bending) demonstrate the application of rapid local heating. However, for bulk forming, the fact that actuation can be applied only at the surface, limits the spatial gradients of strain, strain rate and temperature that can be applied to the core of the workpiece. This restriction can be overcome only by reducing workpiece dimensions – so a potential benefit from developing nearer-net shape processes may be that forming workpieces with reduced thickness may allow more control of internal microstructure.

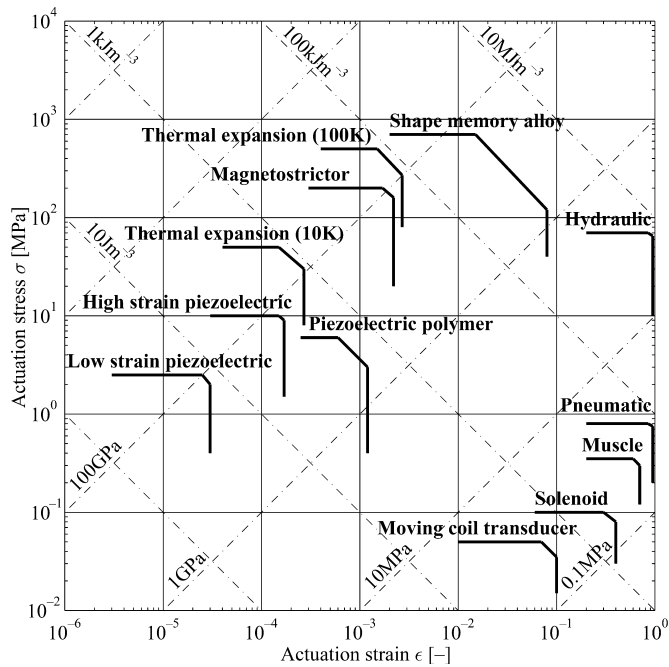


**Fig. 4.** Actuator stress vs. strain for various linear mechanical actuators. From Huber et al. (1997) by permission of the Royal Society.

## 5.2. Actuator positioning

The number and positioning of actuators in a process define its spatial controllability – the extent to which deviations (errors)

between actual and target workpiece states can be corrected. In simple cases, this error can be described as a scalar. For example, the target of L-bending is to achieve a specified bend angle, so Yang et al. (1998) could use a single displacement actuator to provide sufficient control for this scalar error. However, if the error is more distributed, more flexibility is required to control the error. For example, Fig. 5a shows a possible form that the error might take over a line (this might represent the error curvature along the length of a section, for example). The actuator with the response in Fig. 5b would not be able to control this error so additional flexibility may be created with a series of actuators (Fig. 5c) or using a single, mobile actuator (Fig. 5d).

Arrays of actuators, such as in Fig. 5c, have been used in strip rolling and stamping. Spooner and Bryant (1976) describe strip rolling with an array of bending jacks and thermal actuators to alter the shape of the work roll to control the thickness in the cross-direction, while Li et al. (2007) describe a stamping process using a matrix of punches to make a flexible die/punch set. Spooner and Bryant's approach was extended by Duncan et al. (1998), who characterise both the error in strip profile and the response of each actuator using a basis set of Chebyshev polynomials. They show that in order to control higher-order errors, an increased set of actuators with higher-order responses is required. In addition, if two actuators have similar responses and act over the same area, the controller would become ill-conditioned.

Mobile actuators are used in spinning, laser forming and many new flexible processes including incremental sheet forming. Such designs require fewer actuators, and avoid the limitations of arrays of actuation, but at the cost of slower processing: Hao and Duncan (2011) report that each forming step in closed-loop incremental sheet forming may take up to 40 s, and that 25 such steps might be needed to form a complete part, in comparison of stamping cycles of

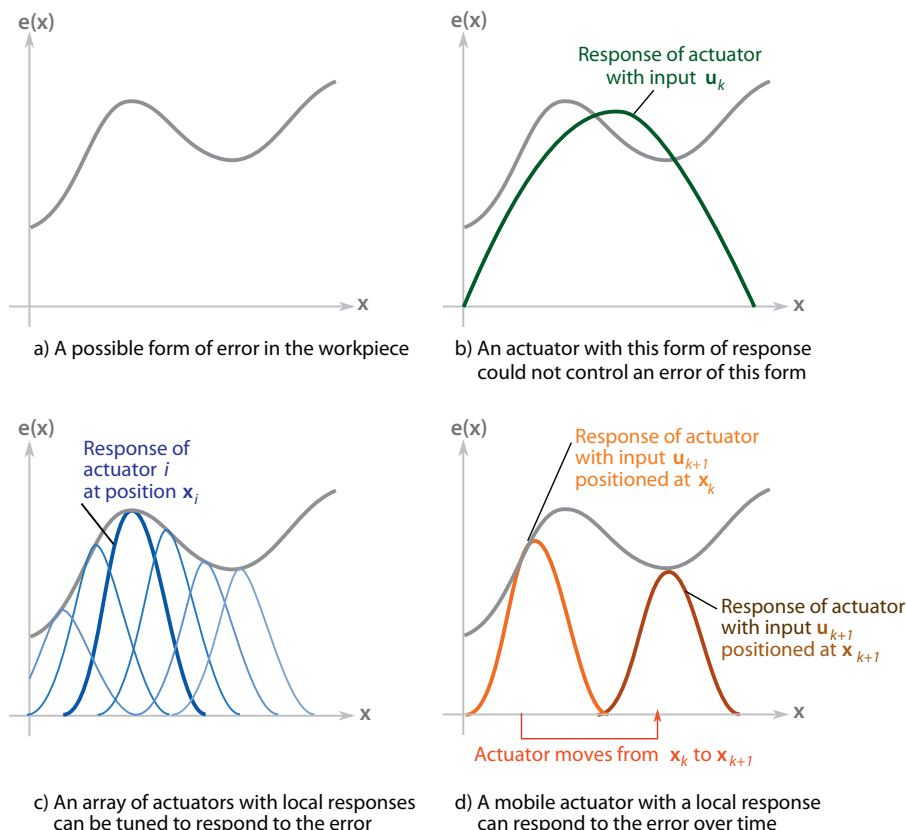


**Fig. 5.** A possible form of the error in state (a) and responses with various actuators (b–d).

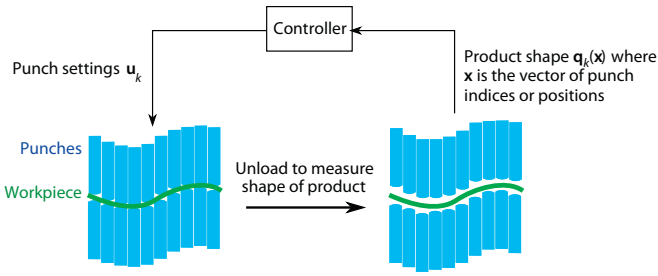


Fig. 6. Stamping with a matrix of punches.

Adapted from Li et al. (2007).

one second. However, in a dynamic, thermal process (such as heat treatment), Demetriou et al. (2003) showed that having a mobile thermal actuator allowed more flexibility in the control of temperature distribution, and also achieved the required temperature distribution more rapidly than possible with a single fixed actuator.

## 6. Process model development for closed-loop control

The minimisation required in both open-loop (Eq. (7)) and closed-loop (Eq. (11)) controllers requires a process model and usually also includes constraint inequalities. In both cases, the minimisation is over all possible tool-paths, so the process model and constraint inequalities will be evaluated many times. In open loop control, the minimisation is performed off-line, so solution times of hours or days may be acceptable. However, any model error will degrade the resulting product properties, and will influence the application of the process constraints. In contrast, in closed loop control, model errors can to some extent be tolerated as sensing provides regular updates to the estimated workpiece state. However, because the closed loop minimisation (Eq. (11)) is performed online, a fast model is required.

The requirement for accurate models in open loop control has led to the continued development of modelling techniques for metal forming since the start of the 20th century. Osakada (2010) reviews the history of this development, noting a number of methods, such as slip-line fields, upper bound analysis and slab methods, that could be used to generate approximate analytical models. However, Osakada concludes that with the exponential increase in computing power since the 1970s, the Finite Element Method (FEM) has been dominant since the 1990s.

Despite today's computing power, FE models remain computationally expensive, and for most processes could not at present be used online in closed loop control systems. Even in open loop control systems, they often lack sufficient accuracy to achieve typical production tolerances in the final product. For this reason, researchers have made other approximations to develop fast, closed-form process models.

The fastest and most approximate models used in closed-loop control of product properties are linear, discrete-time, quasi-static, and assume that the process model is spatially and time invariant. In addition, the controller often uses a control horizon of one time step to minimise the computational cost of each minimisation. For example, Hardt and Webb (1982) designed a closed loop control system for the shape of a part stamped with a matrix of punches (Fig. 6). They use a conservative model of springback based on the difference between the tool shape and the resulting part shape. Thus, the control actions are given by,

$$\mathbf{u}_k = \mathbf{u}_{k-1} - [\hat{\mathbf{q}}_k(\mathbf{x}) - \mathbf{q}_k(\mathbf{x})] \quad (12)$$

Despite the conservative modelling of springback, as well as the implicit assumption that each punch has the same response, a reduction of error from 13% to 2% (a factor of 6.5) was achieved in

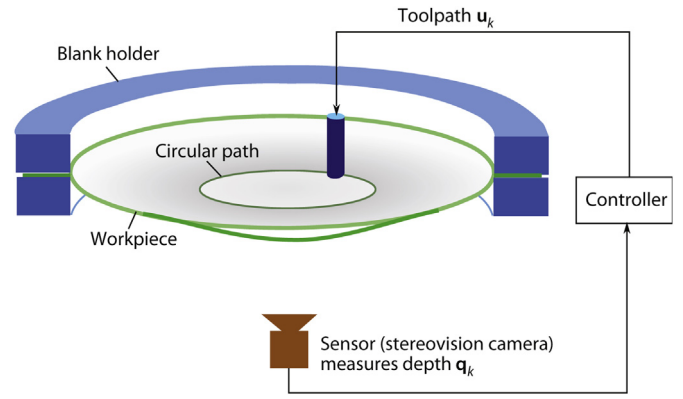


Fig. 7. Incremental sheet forming.

5 iterations. However, Li et al. (2007) reduced the error faster (from 4.2 to 0.25 mm (a factor of 17) in the same number of iterations) by scaling the error term in Eq. (12) as:

$$\mathbf{u}_k = \mathbf{u}_{k-1} - \mathbf{c}_k(\mathbf{x})[\hat{\mathbf{q}}_k(\mathbf{x}) - \mathbf{q}_k(\mathbf{x})] \quad (13)$$

For processes with mobile tools, in addition to actuator intensity, the tool path must be controlled. For example, Allwood et al. (2009) and Hao and Duncan (2011) applied closed-loop control to incremental sheet forming (ISF) of axisymmetric parts (Fig. 7), restricting the tool path to a series of circular contours with constant tool indentation along each contour. Allwood et al. (2009) determine the indentation in each step using an impulse response approach, having determined the impulse response experimentally at three stages in the process (early, middle and late). Hao and Duncan (2011) linearised the process model about a planned tool path, to create a fast online process model:

$$\begin{aligned} \mathbf{q}_{k+1} &= \hat{\mathbf{q}}_{k+1} + (\mathbf{q}_k - \bar{\mathbf{q}}_k) + \mathbf{B}_k(\mathbf{u}_k - \bar{\mathbf{u}}_k) \text{ with } \mathbf{B} \text{ defined so that } \mathbf{B}_k \bar{\mathbf{u}}_k \\ &= \bar{\mathbf{q}}_{k+1} - \bar{\mathbf{q}}_k \end{aligned} \quad (14)$$

where the bars indicate the planned actuation and workpiece state.

In laser bending, Edwardson et al. (2004) took a similar approach for non-axisymmetric products, using contours of error between the target and measured product height as a path for the laser, with the same impulse response as above to determine actuation intensity.

These process models relate to discrete processes, in which a single part is made in a number of steps, with measurements and control updates between each step. However, in continuous processes such as strip rolling or roll forming, some material must be run out of the forming zone before it can be measured and before the actuator settings can be changed, creating a delay between actuation and sensing. In strip rolling (Fig. 8), Duncan (1997) exploit this delay to determine the open-loop response of the actuators from small perturbations in their settings, and Duncan et al. (1998) use a zero-order-hold approach to this delay, so after the actuator settings are changed the system waits for a steady state to be reached before taking another measurement and generating another set of control actions.

The discrete, zero-order-hold approach to controlling strip rolling neglects the dynamic effects of the changes to the actuator settings. Duncan (1995) justifies this assumption, pointing out that in many cases the dynamic effects and the steady state response are separable if all actuators have the same dynamic response and if, in the transient stage, the response retains the same shape but simply changes amplitude. For actuators with slower dynamic responses, such as those based on thermal expansion, the control system can be designed to compensate for the actuator dynamics (Duncan, 1989). Wellstead et al. (2000) show that in order to achieve high

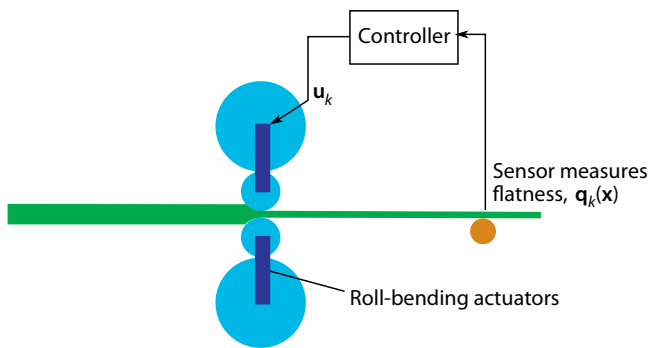


Fig. 8. Strip rolling.

accuracy over small areas (i.e. constant thickness over small areas of sheet), then the delay in the response must be reduced by moving the actuators and sensors closer together and by increasing the response speed of actuators. However, by doing this, they show that often the process model can no longer be separated into steady-state and transient responses, and a full 2-dimensional model is required.

Luo et al. (1996) use a dynamic continuous process model to control the multi-axis beam bending process illustrated in Fig. 9. They determine an approximate transfer function in Laplace space (transformed from the time-domain) based on classical beam theory with an elastic-perfectly-plastic material model. However, they note that with a dynamic model there is a chance that the system might become unstable.

Li et al. (2007) employed an adaptive model, to attempt to counter this instability by refining the process model using the history of inputs and outputs from earlier in the process. However, when Sun and Stelson (1997) used an adaptive process model to control multi-axis bending, they found that there were zeros in the right hand plane of the resulting transfer function which would result in unstable poles when inverted. They therefore used the method proposed by Gross et al. (1994) to cancel the unstable pole using a feed-forward controller.

The closed form process models given above are fast, but are not available for all metal forming processes. In order to take advantage of the flexibility and accuracy of FE modelling with the speed of these linear models, Prud'homme et al. (2002) ran (computationally expensive) FE models offline at different points in state space, and then interpolated between them online to provide real-time solutions. However, the interpolation is only valid over the region of state space modelled.

Some researchers, therefore, have used empirical process models to control metal forming processes. For example, Hardt et al. (1982) applied closed-loop control of product properties to a three-roll bending process, while Hardt and Hale (1984) did the same for three-roll straightening. Rather than explicitly using a process

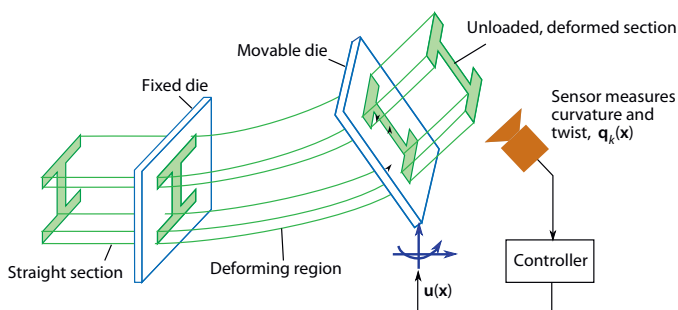


Fig. 9. Multi-axis bending and twisting.

Adapted from Sun and Stelson (1997).

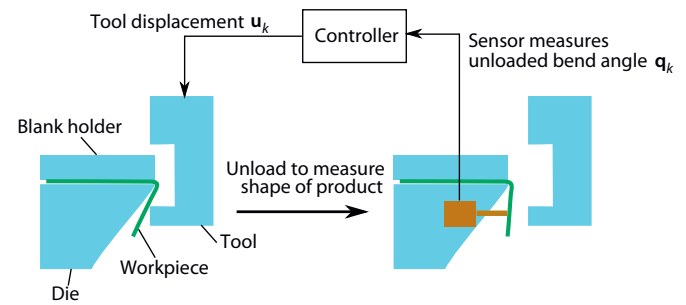


Fig. 10. L-bending.

Adapted from Yang et al. (1998).

model to determine the evolution of the actuator settings, they used an integrator to control the actuator. This is a sub-set of proportional-integral-differential (PID) controllers, which are criticised by Desborough and Miller (2002) as they require retuning when process conditions change, but this is often neglected. They are often used, nevertheless, for their ease of set-up and use.

In a more advanced example of an empirical process model, Yang et al. (1998) applied closed-loop control of product properties to a flexible L-bending process (Fig. 10). By measuring the angle of the bend after the initial attempt at L-bending, the machine over-bends the workpiece in order to compensate for the springback. Rather than using a process model to determine the actuator controls they use a neural network. The network compares the input and state following the initial bend to results of previous experiments in order to determine the optimal actuator settings for the current workpiece.

Despite extensive work on developing fast process models for closed-loop control, few authors have focused on evaluating constraints, even though Model Predictive Control described in Section 2 is particularly suited to handling them. The exception is in deep drawing (Fig. 11), where the blank holder pressure must be set in order to avoid failure due to wrinkling or tearing.

Siebert et al. (2000) and, more recently, Lim et al. (2008) reviewed the different approaches researchers have taken to predict such failures and found that in all approaches so far the blank holder force has been controlled to maintain a measured state variable within a given trajectory – in non-axisymmetric deep drawing the blank holder force distribution can be controlled with a segmented blank holder (Siebert et al., 2000) or draw beads. In the cases reviewed by Siebert et al. and Lim et al. the state was the

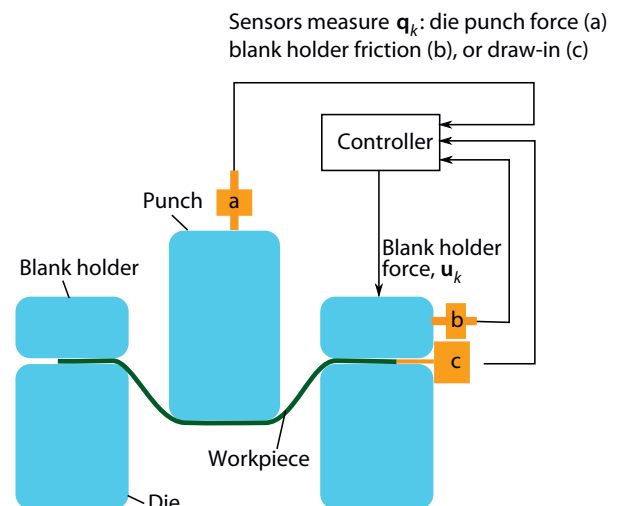
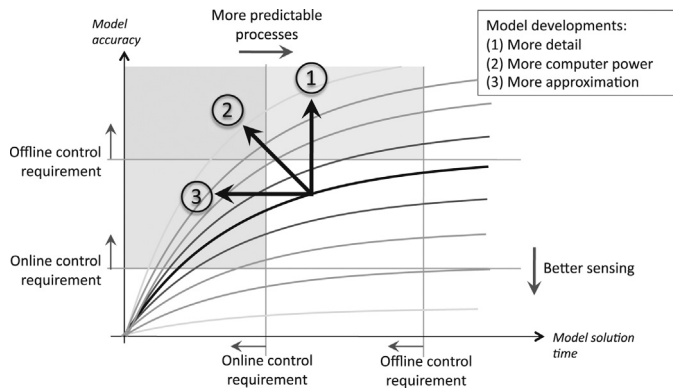


Fig. 11. Deep drawing.





**Fig. 12.** The trade-off between model solution time and model accuracy in developing models for open and closed loop control.

punch force, blank holder friction or flange draw-in. More recently, [Blaich and Liewald \(2008\)](#) measure the wall stress with a newly designed sensor and use this as the state. Successful trajectories of these states were found by experiment, so only some disturbances such as changes in lubrication conditions and eccentric blank loading could be tolerated. [Hardt and Fenn \(1993\)](#) note that changes to the thickness and material properties of the blank must be known a priori if trajectories of punch force or blank holder friction are followed, while following flange draw-in can tolerate these disturbances without prior knowledge.

In all the examples reviewed in this section, approximations have been used to speed up the solution of the process model and constraints. Future expansion of the application of closed-loop control requires more development of faster approximate models, and the opportunity for this development is illustrated in [Fig. 12](#).

To date, the developers of process models have been pre-occupied with accuracy rather than increasing speed. [Osakada's \(2010\)](#) review of modelling techniques showed that since the initial development of plasticity theory in the 19th century, the development of process modelling tools have become more detailed and accurate, and concludes that detailed FEM is the dominant tool for process modelling today. This is reflected in the movement of process models in [Fig. 12](#) upwards, further into the region of open-loop feasibility. Some authors have focused on developing less detailed but faster models. For example, [Bramley \(2001\)](#) reviews his own work in developing the upper bound element technique (UBET), while [Alfozan and Gunasekera \(2003\)](#) used this method to design tools for ring rolling processes, and found that a UBET analysis took minutes compared to FEM which would have taken weeks. [Samolyk and Pater \(2004\)](#) ran an automated slip-line field analysis on closed-die forging, and found that their results were within 20% of the results from FEM, but the analysis only took 1/10 of the time. Although none of these examples have been used in closed loop control of product properties, the benefit of faster but more approximate models is reflected by process models in [Fig. 12](#) moving from right to left, further into the region where closed loop control is feasible.

## 7. The future of closed-loop control of product properties

The review of closed-loop control of product properties reported in this paper has revealed applications for controlling errors in geometry and residual stress, and to avoid defects. Furthermore, closed-loop control has the potential to improve material properties and, in future, may be used to control surface properties and

**Table 8**  
Possible future examples of closed-loop control of product properties.

Property	Near-term opportunities
Geometry	<i>Spinning:</i> Overcoming springback, both axisymmetric and asymmetric (due to anisotropy in the material)
Surface properties	<i>Ring rolling:</i> Overcoming form errors <i>Extrusion:</i> Overcoming surface and internal defects in flexible extrusion (e.g. the variable depth extruder developed by <a href="#">Makiyama and Murata, 2005</a> ), by changing the temperature gradients and flow pattern upstream.
Material properties	<i>Incremental Forging:</i> <a href="#">Recker et al.'s (2011)</a> have designed an observer for estimating material properties in incremental forging, but have not yet shown a working closed-loop controller. However, as computational power improves, the same theory as used in the observer could be used to determine the optimal control actions. This approach could also be applied to other bulk and sheet forming processes.
Damage	<i>Deep drawing:</i> <a href="#">Hsu et al. (2002)</a> reviewed deep drawing processes where the blank holder force is controlled so that the punch force, friction force, or draw-in follows a pre-defined trajectory. However, with more advanced damage modelling, these trajectories could be adapted online, to allow an approach similar to that applied to flexible incremental deep drawing by <a href="#">Shima et al. (1999)</a> <i>Spinning:</i> Toolpath design in spinning is currently performed off-line, typically by a skilled craftsman. If damage can be monitored and controlled using fast models, the toolpath could be adapted or generated online.

damage. [Table 8](#) illustrates some possible opportunities to develop new closed-loop control processes.

Future expansion in the applications of closed-loop control (particularly in the areas of surface properties, materials properties and damage) requires faster process models that can be run online. This is demonstrated by the work of [Recker et al. \(2011\)](#) on the use of closed-loop control of material properties. There are two possible approaches to increase the speed of process models: to focus development of process modelling on speed, rather than detail and accuracy; or to develop more predictable processes.

Designing more predictable forming processes with faster process models is a potential solution which has not received any attention in the published literature. However, this is one of the reasons why machining is so popular as a flexible manufacturing process: it is very predictable, as material is removed only at the tool location. Toolpath generation for machining is thus much simpler than for forming, and many computer software packages already exist for doing this very quickly. If a predictable forming process were designed, similar packages could create toolpaths for forming online, just as quickly. In [Fig. 12](#), this would be the equivalent of relaxing the requirement for modelling speed, and therefore moving the online control speed requirement from left to right.

Computing power is meanwhile growing exponentially as Moore's law continues to hold true. Ongoing advances in computing power will allow increasingly detailed online process observation, modelling and control. Furthermore, designers continue to demand both tighter tolerances and increased flexibility, and production managers continue to push tailored production scheduling to respond to market demand. Both of these factors will further enhance the possibilities of and the demand for closed-loop control of product properties to overcome uncertainties and disturbances in increasingly flexible metal forming processes.



## Acknowledgements

The first author is funded by Siemens Metals Technologies and the EPSRC Doctoral Training Account.

## Appendix A. Descriptions of Sensors

Table A.1 Description of Displacement Sensors

<b>Mechanical Follower</b>	A roller or point moves into contact with the part, or remains in contact and follows the surface of the part as it changes. The position of the roller or point is then measured with a Linear Variable Differential Transformer (LVDT).
<b>Direct Induction</b>	The inductance of a coil changes as the edge of metal moves over it. The inductance can be measured and used to determine the position of the edge of the sheet.
<b>Laser Line Triangulation</b>	A line is projected onto the part by a laser. The orientation is measured using a camera, and triangulation is used to determine the orientation of the surface.
<b>Silhouette (single)</b>	Place part in front of light, and take silhouette in order to measure outline of shape (Dworkin and Nye, 2006).
<b>Laser scanning</b>	The surface is scanned by a laser displacement sensor to measure the distance from the sensor to each point.
<b>Stereovision Camera</b>	Two cameras are used to generate a 3D image of the surface of a part.
<b>Silhouette (series, as part rotated)</b>	As above, but gradually rotate the part and take a series of silhouettes in order to build up a 3D image of the surface (Goldstein et al., 1985).
<b>X-ray Tomography</b>	X-ray techniques are used to take multiple cross-sections of the part. These cross sections are then put together to make a 3D image of the part. This also gives information of internal defects and density (Broughton and Nunn, 2006).

Table A.2 Descriptions of surface roughness/defect sensors from Whitehouse (1994), Broughton and Nunn (2006), and Kalpakjian and Schmid (2008)

<b>Stylus Scanners</b> <i>Including scanning microscopes</i>	The difference in height between the surface and a reference surface is measured either with a mechanical follower, or a scanning microscope (e.g. tunnelling, force). Whitehouse argued that these methods are similar on grounds of functionality. Even if scanning microscopes do not require contact, they still operate extremely close to the surface. The tool is usually rastered over the surface to build up a 3D image.
<b>Optical Surface Measurement</b>	A laser light is shone on the surface, and effects such as reflection, interference, focus etc. are used to infer information about the surface texture. This can measure at a point, and be rastered over a surface, or a laser line can be used to measure along a line.
<b>Capacitance Techniques</b>	The capacitance between a probe and the surface is measured, and can be related to the distance between them.
<b>Acoustic Emissions Measurement</b>	A tool is dragged over a surface, generating a noise which is dependent on the surface roughness. By measuring the noise, the roughness can be calculated.
<b>Optical Microscopy</b>	The surface is viewed with an optical microscope in order to identify the position of defects.

## Stereo Optical Microscopy

Two optical microscopes are used to build up a full, 3D image of a surface.

## Scanning Electron Microscopy

A beam of electrons are projected onto and scanned across the surface. The primary and secondary electrons which return are detected, and used to build up a 3D image of the surface.

## Liquid-penetrants Technique

A penetrating die is placed on the surface and is allowed to penetrate into defects etc. Excess is wiped off and a developer is used to bring out the die, in order to highlight the presence of defects.

## Inductive Technique

Some correlation between mutual inductance of the surface and a probe, and surface roughness was found, but this only provides comparative measures of roughness.

## Impedance/Skin Effect Technique

At high frequency, impedance is due to the skin effect. The frequency can be increased until the skin thickness is the same order of the surface roughness. At this point, the impedance will increase. This will characterise the surface roughness.

## Friction Measurement

The friction between two surfaces is dependent on their roughness. The friction force can therefore be measured, and used to determine the roughness.

Table A.3 Descriptions of force sensors from Shieh et al. (2001)

<b>Load cell</b> <i>Including load bolts.</i>	Load cells are placed in the path of the load, and output an electrical signal in proportion to the force transferred through the load cell, either using a strain gauge or hydraulic pressure.
<b>Piezoelectric (PE) Force Sensor</b>	In passive mode, PE force sensors convert force directly into electrical signal. In active mode, their oscillation frequency varies with mechanical loading. Both of these effects can be measured and related to the load.
<b>Piezoresistive (PR) force sensors</b>	PR force sensors' resistance changes with applied force.
<b>Tactile Sensors</b>	An array of other force sensors or displacement sensors is used in order to measure a contact force or deflection profile.

Table A.4 Description of temperature sensors from Shieh et al. (2001)

<b>Thermocouple</b>	A thermocouple is a junction between two metals. A temperature change results in a voltage across the junction. Yoneyama and Tozawa (1990) placed two thermocouples at different depths in a tool, and used the measurements to infer the heat flow, and therefore the temperature and tool tip of the tool, and thus the temperature on the workpiece.
<b>Bimetallic thermometers</b>	Two metals of different thermal expansion are attached. When the temperature changes, the differential expansion caused bending of the strip, which can be measured.
<b>Fibre-optic temperature sensors</b>	Relies on the dependence on temperature of optical effects including fluoroptic, interferometric and light absorption effects, which can be measured.
<b>Integrated-circuit (IC) temperature sensors</b>	Measures the change in characteristic of a pn-junction in a diode, which is dependent on temperature.
<b>Irreversible/change-of-state temperature sensors</b>	These rely on a change of state of a material or coating, leading to a change in appearance which indicates a temperature has been reached. These are irreversible.

<b>Liquid crystal temperature indicators</b>	The molecular order of liquid crystals change with temperature, although typically only 7–16 temperatures levels can be indicated. This changes the optical properties such as colour, which can be measured.
<b>Liquid-in-glass thermometers</b>	Rely on the thermal expansion of liquid. The volume of liquid is measured and related to the temperature.
<b>Piezoelectric (PE) temperature sensors</b>	Rely on the change of oscillation frequency with temperature of piezoelectric materials. The frequency can be measured and related to temperature.
<b>Thermistors</b>	Rely on the change in resistance of material with temperature. This can be measured and related to the temperature.
<b>Thermostats</b> <i>Bimetallic and gas/vapour actuated</i>	A switch is actuated (reversibly, although usually with hysteresis) when a certain temperature is reached.
<b>Optical pyrometer</b> <i>e.g. infrared thermometer/camera</i>	The intensity of radiation from the part is measured, and used to infer the temperature.

Table A.5 Description of defect, microstructure and material properties sensors from (Kalpakjian and Schmid, 2008) and (Broughton and Nunn, 2006)

<b>Magnetic-particle inspection technique</b>	Small ferromagnetic particles are placed on the surface. The part is magnetized, causing these particles to arrange themselves. The will arrange themselves around defects, highlighting their presence.
<b>Thermography</b>	The part is heated, and then the temperature is recorded as it cools. By monitoring the subsequent cooling, surface and subsurface defects can be detected.
<b>Optical Microscopy</b>	A magnified image of the surface is taken and, with appropriate lighting, individual grains can be identified and measured. The composition may also be identified by the colour.
<b>Eddy-current inspection techniques</b>	The part is placed in an oscillating electromagnetic field, inducing eddy currents. The presence of defects change the eddy currents, allowing them to be picked up by changes in the electromagnetic field.
<b>Induction spectroscopy</b>	The magnetic properties of steel depend on the microstructure. These magnetic properties can be measured by exposing the material to high frequency electromagnetic fields and measuring the resulting flux density and field strength, and can then be related back to the microstructure. The microstructure can be measured at different depths by varying the frequency of the electromagnetic field.
<b>Radiography and Tomography</b> <i>e.g. X-Ray, Photon, Neutron</i>	These three radiography techniques can be used to generate an image of the part which reveals density changes and flaws.
<b>X-ray Diffraction (XRD)</b>	X-rays are projected onto a part. The crystal structure of the material causes the X-rays to diffract, resulting in diffraction peaks and troughs. The location of these peaks and troughs can be measured and related to the crystal structure. With knowledge of elastic properties, this can also give information on residual stresses.

<b>Ultrasonic/Acoustic methods</b>	Defects reflect the ultrasonic beams. These reflections can be detected, and their timing and amplitude indicate the presence and location of the defect. The speed and attenuation of the sound waves give information about the elastic properties. The scattering characteristics can be used to determine grain size.
<b>Acoustic-emission</b>	The formation of defects, plastic deformation, phase transformation and reorientation of grain boundaries generate acoustic signals which can be detected.

## References

- Alfozan, A., Gunasekera, J.S., 2003. Upper Bound Element Technique (UBET) as a Design Tool for Ring Rolling Process., pp. 1–17.
- Allwood, J.M., 2007. A structured search for novel manufacturing processes leading to a periodic table of ring rolling machines. *J. Mech. Des.* 129, 502.
- Allwood, J.M., 2008. A structured search for new metal forming processes. In: *International Conference on Technology of Plasticity*, pp. 1–6.
- Allwood, J.M., Music, O., Raithathna, A., Duncan, S.R., 2009. Closed-loop feedback control of product properties in flexible metal forming processes with mobile tools. *CIRP Ann. Manuf. Technol.* 58, 287–290.
- Allwood, J.M., Utsunomiya, H., 2006. A survey of flexible forming processes in Japan. *Int. J. Mach. Tools Manuf.* 46, 1939–1960.
- Astrom, K.J., Murray, R.M., 2008. *Feedback Systems*. Princeton University Press.
- Blaich, C., Liewald, M., 2008. New approach for closed-loop control of deep drawing processes. In: Liewald, M. (Ed.), *New Developments in Sheet Metal Forming 2008*. Fellbach, Frankfurt, Germany, pp. 363–384.
- Bramley, A., 2001. UBET and TEUBA: fast methods for forging simulation and preform design. *J. Mater. Process. Technol.* 116, 62–66.
- Bravington, C.A., Barry, D.C., McClure, C.H., 1976. Design and development of a shape control system. In: *The Metals Society Shape Conference*, Chester, pp. 82–88.
- Cao, J., Junghoon, L., Peshkin, M., 2002. Real-time draw-in Sensors and Methods of Fabrication.
- Cao, J., Kinsey, B., Solla, S., 2000. Consistent and minimal springback using a stepped binder force trajectory and neural network control. *ASME J. Eng. Mater. Technol.* 122, 113–118.
- Clark, D.E., Sutton, W.H., 1996. Microwave processing of materials. *Annu. Rev. Mater. Sci.* 26, 299–331.
- Curtain, R.F., Zwart, H., 1995. *An Introduction to Infinite-Dimensional Linear Systems Theory*. Springer.
- Davis, C.L., Strangwood, M., Peyton, A.J., 2011. Overview of non-destructive evaluation of steel microstructures using multifrequency electromagnetic sensors. *Ironmaking & Steelmaking*, Maney Publishing 38, 8.
- Demetriou, M.A., Paskaleva, A., Vayena, O., Doumanidis, H., 2003. Scanning actuator guidance scheme in a 1-d thermal manufacturing process. *IEEE Trans. Contr. Syst. Technol.* 11, 757–764.
- Desborough, L., Miller, R., 2002. Increasing customer value of industrial control performance monitoring – Honeywell's experience. *AIChE Symp. Ser.* 98, 169–189.
- Duncan, S.R., (Ph.D. thesis) 1989. *The cross directional control of a web forming process*. Imperial College of Science, Technology and Medicine, London, UK.
- Duncan, S.R., 1995. The design of robust cross-directional control systems for paper making. In: *Proceedings of the 1995 American Control Conference*, Seattle, Washington, pp. 1800–1805.
- Duncan, S.R., 1997. Estimating the response of actuators in a cross-directional control system. *Pulp Paper Canada* 98, 61–64.
- Duncan, S.R., Allwood, J.M., Garimella, S.S., 1998. The analysis and design of spatial control systems in strip metal rolling. *IEEE Trans. Contr. Syst. Technol.* 6, 220–232.
- Duncan, S.R., Allwood, J.M., Heath, W.P., Corscadden, K.W., 2000. Dynamic modeling of cross-directional actuators: implications for control. *IEEE Trans. Contr. Syst. Technol.* 8, 667–675.
- Duncan, S.R., Bryant, G.F., 1997. The spatial bandwidth of cross-directional control systems for web processes. *Automatica* 33, 139–153.
- Edwards, S., Moore, A., Abed, E., McBridge, R., French, P., Hand, D., Dearden, G., et al., 2004. Iterative 3D laser forming of continuous surfaces. In: *27th ICALEO*.
- Endelt, B., Tommerup, S., Danckert, J., 2013. A novel feedback control system – controlling the material flow in deep drawing using distributed blank-holder force. *J. Mater. Process. Technol.* 213, 36–50.
- Frade, M., Enguita, J.M., Álvarez, I., 2012. In situ 3D profilometry of rough objects with a lateral shearing interferometry range finder. *Opt. Laser. Eng.* 50, 1559–1567.
- Geiger, M., Vollertsen, F., 1993. The mechanisms of laser forming. *CIRP Ann. Manuf. Technol.* 42, 301–304.
- Green, M., Limebeer, D.J.N., 2012. *Robust Linear Control*. Dover Publications.

- Groche, P., Beiter, P., Henkelmann, M., 2008. Prediction and inline compensation of springback in roll forming of high and ultra-high strength steels. *Prod. Eng.* 2, 401–407.
- Groche, P., Fritsche, D., Tekkaya, A.E., Allwood, J.M., Hirt, G., Neugebauer, R., 2007. Incremental bulk metal forming. *CIRP Ann. Manuf. Technol.* 56, 635–656.
- Gross, E., Tomizuka, M., Messner, W., 1994. Cancellation of discrete time unstable zeros by feedforward control. *ASME J. Dynam. Syst. Measur. Contr.* 116, 33–38.
- Gururajan, G., Ogale, A.A., 2012. Real-time crystalline orientation measurements during low-density polyethylene blown film extrusion using wide-angle X-ray diffraction. *Polym. Eng. Sci.* 52, 1532–1536.
- Hamedon, Z., Mori, K., Abe, Y., 2012. In-situ measurement of three-dimensional deformation behaviour of sheet and tools during stamping using borescope.
- Hao, W., Duncan, S.R., 2011. Optimization of tool trajectory for Incremental Sheet Forming using closed loop control. In: IEEE International Conference on Automation Science and Engineering, pp. 779–784.
- Hardt, D., 1993. Modeling and control of manufacturing processes: getting more involved. *ASME J. Dynam. Syst. Measur. Contr.* 115, 291–300.
- Hardt, D., Fenn, R., 1993. Real-time control of sheet stability during forming. *J. Eng. Industry* 115, 299–308.
- Hardt, D., Hale, M., 1984. Closed loop control of a roll straightening process. *CIRP Ann. Manuf. Technol.* 33, 137–140.
- Hardt, D., Roberts, M., Stelson, K., 1982. Closed-loop control in a roll bending process. *ASME J. Dynam. Syst. Measur. Contr.* 104, 317–322.
- Hardt, D., Webb, R., 1982. Sheet metal die forming using closed-loop shape control. *CIRP Ann. Manuf. Technol.*
- Hawkyard, J.B., Johnson, W., Kirkland, J., Appleton, E., 1973. Analyses for roll force and torque in ring rolling, with some supporting experiments. *Int. J. Mech. Sci.* 15, 873–893.
- Hsu, C., Ulsoy, A.G., Demeri, M.Y., 2002. Development of process control in sheet metal forming. *J. Mater. Process. Technol.* 127, 361–368.
- Huber, J., Fleck, N.A., Ashby, M.F., 1997. The selection of mechanical actuators based on performance indices. *Proc. Royal Soc. Lond. A: Math. Phys. Eng. Sci.* 2185–2205.
- Jeong, H., Kim, H., Lee, S., Dornfeld, D.A., 2006. Multi-sensor monitoring system in chemical mechanical planarization (CMP) for correlations with process issues. *CIRP Ann. Manuf. Technol.*, 55.
- Jeswiet, J., Micari, F., Hirt, G., Bramley, A., Dufloy, J., Allwood, J.M., 2005. Asymmetric single point incremental forming of sheet metal. *CIRP Ann. Manuf. Technol.* 54, 88–114.
- Koppers, U., (Ph.D. thesis) 1987. Geometrie, kinematik und statik beim walzen von ringen mit rechteckquerschnitten. RWTH, Aachen, Germany.
- Lange, K., 1985. Handbook of Metal Forming. McGraw-Hill.
- Li, M.-Z., Cai, Z.-Y., Liu, C., 2007. Flexible manufacturing of sheet metal parts based on digitized-die. *Robot. Comput. Integr. Manuf.* 23, 107–115.
- Liang, S., Dornfeld, D.A., 1990. Characterization of sheet metal forming using acoustic emission. *J. Eng. Mater. Technol.* 112, 44–51.
- Lim, Y., Venugopal, R., Ulsoy, A.G., 2008. Advances in the control of sheet metal forming. In: 17th World Congress of The international Federation of Automatic Control, pp. 1875–1883.
- Luo, J.X., Joynt, D.L., Stelson, K., 1996. Control of the fabrication of long slender workpieces of arbitrary shape – Part II: Closed-loop control of the multi-axis bending process. *ASME J. Dynam. Syst. Measur. Contr.* 118, 549–556.
- Maciejowski, J.M., 2000. Predictive Control with Constraints. Prentice-Hall.
- Mahayotsanuna, N., Sahb, S., Cao, J., Peshkin, M., Gao, R.X., Wang, C.T., 2009. Tooling-integrated sensing systems for stamping process monitoring. *Int. J. Mach. Tools Manuf.* 49, 634–644.
- Makiyama, T., Murata, M., 2005. A technical note on the development of prototype CNC variable vertical section extrusion machine. *J. Mater. Process. Technol.* 159, 139–144.
- Michler, J.R., Weinmann, K.J., Kashani, A.R., Majlessi, S.A., 1994. A strip-drawing simulator with computer-controlled drawbead penetration and blankholder pressure. *J. Mater. Process. Technol.* 43, 177–194.
- Milford, R.L., Allwood, J.M., Cullen, J.M., 2011. Assessing the potential of yield improvements, through process scrap reduction, for energy and CO<sub>2</sub> abatement in the steel and aluminium sectors. *Resour. Conserv. Recycl.* 55, 1185–1195.
- Nguyen-Thi, H., Salvo, L., Mathiesen, R.H., Arnberg, L., Billia, B., Suery, M., Reinhart, G., 2012. On the interest of synchrotron X-ray imaging for the study of solidification in metallic alloys. *C. R. Phys.* 13, 237–245 (Elsevier Masson SAS).
- Osakada, K., 2010. History of plasticity and metal forming analysis. *J. Mater. Process. Technol.* 210, 1436–1454.
- Osakada, K., Mori, K., Altan, T., Groche, P., 2011. Mechanical servo press technology for metal forming. *CIRP Ann. Manuf. Technol.* 60, 651–672.
- Pasadas, D., Ramos, H.G., Alegria, F., 2011. Handheld Instrument to detect defects in conductive plates with a planar probe. In: IEEE Instrument and Measurement Technology Conference.
- Prud'homme, C., Rovas, D.V., Veroy, K., Machiels, L., Maday, Y., Patera, A.T., Turinici, G., 2002. Reliable real-time solution of parametrized partial differential equations: reduced-basis output bound methods. *J. Fluids Eng.* 124, 70.
- Recker, D., Franzke, M., Hirt, G., 2011. Fast models for online-optimization during open die forging. *CIRP Ann. Manuf. Technol.* 60, 295–298.
- Rzepniewski, A., Hardt, D., 2008. Development of general multivariable run-by-run control methods with application to a sheet metal forming process. *Int. J. Mach. Tools Manuf.* 48, 599–608.
- Samolyk, G., Pater, Z., 2004. Application of the slip-line field method to the analysis of die cavity filling. *J. Mater. Process. Technol.* 153–154, 729–735.
- Saotome, Y., Okamoto, T., 2001. An in-situ incremental microforming system for three-dimensional shell structures of foil materials. *J. Mater. Process. Technol.* 35, 1323–1640.
- Sheppard, T., Roberts, J.M., 1973. Shape control and correction in strip and sheet. *Int. Metall. Rev.* 18, 1–11.
- Shieh, J., Huber, J., Fleck, N.A., Ashby, M.F., 2001. The selection of sensors. *Prog. Mater. Sci.* 46, 461–504.
- Shima, S., Kotera, H., Kamitani, K., 1999. A fundamental study of incremental deep drawing process. In: Proceedings of the Second IEEE International Conference on Intelligent Processing and Manufacturing of Materials, pp. 565–570.
- Siebert, K., Häussermann, M., Haller, D., Wagnert, S., Ziegler, M., 2000. Tendencies in presses and dies for sheet metal forming processes. *J. Mater. Process. Technol.* 98, 259–264.
- Siebert, K., Ziegler, M., 1997. Closed loop control of the friction force. Deep drawing process. *J. Mater. Process. Technol.* 71, 126–133.
- Spooner, P., Bryant, G., 1976. Analysis of shape and discussion of problems of scheduling set-up and shape control. In: The Metals Society Shape Conference, Chester, pp. 19–29.
- Sun, W., Stelson, K., 1997. System identification and adaptive control of the multi-axis bending and twisting process. *ASME J. Dynam. Syst. Measur. Contr.* 119, 782–790.
- Sunseri, M., Cao, J., Karafillis, A.P., Boyce, M., 1996. Accommodation of springback error in channel forming using active binder force control: numerical simulation and experiments. *ASME J. Eng. Mater. Technol.* 118, 426–435.
- Takada, H., Tomura, Y., Aratani, M., Yamasaki, T., Sasaki, T., 2011. On-line detection system for internal flaws in as-hot-rolled steel strip using ultrasonic probe array. *Mater. Trans.* 52, 531–538.
- Viswanathan, V., Kinsey, B.L., Cao, J., 2003. Experimental implementation of neural network springback control for sheet metal forming. *ASME J. Eng. Mater. Technol.* 125, 141–147.
- Wellstead, P.E., Zarrop, M.B., Duncan, S.R., 2000. Signal processing and control paradigms for industrial web and sheet manufacturing. *Int. J. Adapt. Contr. Signal Process.* 14, 51–76.
- Xiaokai, W., Lin, H., 2011. On-line measurement method for various guide modes of vertical ring rolling mill. *Measurement* 44, 685–691.
- Yang, M., Manabe, K., Nishimura, H., 1998. Development of an intelligent tool system for flexible L-bending process of metal sheets. *Smart Mater. Struct.* 7, 530–536.
- Yang, M., Shima, S., Watanabe, T., 1990. Model-based control for three-roll bending process of channel bar. *J. Eng. Industry* 112, 346–351.
- Yogo, Y., Takeuchi, H., Tanaka, K., Iwata, N., Nakanishi, K., Ishikawa, T., 2009. MRT letter: in situ observation method for microstructural changes of steel during hot deformation. *Microsc. Res. Tech.* 72, 899–901.
- Yoneyama, T., Tozawa, Y., 1990. Direct Measurement of Stress and Heat between Work and Tool in Metal Forming. *CIRP Ann. Manuf. Technol.* 39, 219–222.
- Yun, J.S., Cho, H.S., 1985. Suboptimal design approach to the ring diameter control for ring rolling process. *ASME J. Dynam. Syst. Measur. Contr.* 107, 207–212.
- Zhang, H., Murata, M., Suzuki, H., 1995. Effects of various working conditions on tube bulging by electromagnetic forming. *J. Mater. Process. Technol.*